Am J Physiol Regul Integr Comp Physiol 296: R929–R935, 2009.
First published February 11, 2009; doi:10.1152/ajpregu.90824.2008.

Adiponectin is required to mediate rimonabant-induced improvement of insulin sensitivity but not body weight loss in diet-induced obese mice

Stéphanie Migrenne,[1] Amélie Lacombe,[1] Anne-Laure Lefèvre,[1] Marie-Pierre Pruniaux,[2] Etienne Guillot,[2] Anne-Marie Galzin,[2] and Christophe Magnan[1]

[1]*University Paris-Diderot, Centre National de la Recherche Scientifique, Paris, France; and* [2]*Sanofi-Aventis Research and Development, Rueil-Malmaison, France*

Submitted 9 October 2008; accepted in final form 3 February 2009

Migrenne S, Lacombe A, Lefèvre AL, Pruniaux MP, Guillot E, Galzin AM, Magnan C. Adiponectin is required to mediate rimonabant-induced improvement of insulin sensitivity but not body weight loss in diet-induced obese mice. *Am J Physiol Regul Integr Comp Physiol* 296: R929–R935, 2009. First published February 11, 2009; doi:10.1152/ajpregu.90824.2008.—The increase in adiponectin levels in obese patients with untreated dyslipidemia and its mRNA expression in adipose tissue of obese animals are one of the most interesting consequences of rimonabant treatment. Thus, part of rimonabant's metabolic effects could be related to an enhancement of adiponectin secretion and its consequence on the modulation of insulin action, as well as energy homeostasis. The present study investigated the effects of rimonabant in adiponectin knockout mice ($Ad^{-/-}$) exposed to diet-induced obesity conditions. Six-week-old $Ad^{-/-}$ male mice and their wild-type littermate controls ($Ad^{+/+}$) were fed a high-fat diet for 7 mo. During the last month, animals were administered daily either with vehicle or rimonabant by mouth (10 mg/kg). High-fat feeding induced weight gain by about 130% in both wild-type and $Ad^{-/-}$ mice. Obesity was associated with hyperinsulinemia and insulin resistance. Treatment with rimonabant led to a significant and similar decrease in body weight in both $Ad^{+/+}$ and $Ad^{-/-}$ mice compared with vehicle-treated animals. In addition, rimonabant significantly improved insulin sensitivity in $Ad^{+/+}$ mice compared with $Ad^{+/+}$ vehicle-treated mice by decreasing hepatic glucose production and increasing glucose utilization index in both visceral and subcutaneous adipose tissue. In contrast, rimonabant failed to improve insulin sensitivity in $Ad^{-/-}$ mice, despite the loss in body weight. Rimonabant's effect on body weight appeared independent of the adiponectin pathway, whereas adiponectin seems required to mediate rimonabant-induced improvement of insulin sensitivity in rodents.

endocannabinoid system; cannabinoid receptor 1 antagonist; metabolic syndrome

THE DISCOVERY OF THE ENDOCANNABINOID system has led to the development of new treatments for patients with obesity and associated cardiometabolic risk factors (33). Basic research has demonstrated that such a system plays an integrative role in the control of food intake, metabolism, and fat storage through cannabinoid receptors 1 (CB1) located in both the brain and the periphery, notably in adipose tissue (18, 21). Regarding their central effects, endogenous cannabinoids anandamide and 2-arachidonoyl glycerol (2AG) stimulate appetite and food intake in both rodents (8, 10) and humans (13), and CB1 receptor knockout (KO) mice are resistant to diet-induced obesity (23). The role of the peripheral endocannabinoid system in human obesity is also being extensively investigated. Circulating levels of anandamide and 2AG are increased in obese compared with control subjects (7), whereas CB1 mRNA expression is correlated with visceral fat mass (2), thus suggesting an upregulated peripheral endocannabinoid system in human obesity. Rimonabant, the first selective CB1 antagonist, has been shown to reduce fat mass and improve multiple cardiometabolic risk factors in overweight/obese patients, as evidenced in the "Rimonabant In Obesity" (RIO) program (24, 30). One of the most interesting consequences of rimonabant treatment was the increase in plasma adiponectin concentrations in obese patients with untreated dyslipidemia (5), as well as an increased adiponectin mRNA expression in adipose tissue of obese *fa/fa* rats and diet-induced obese (DIO) mice (11) and in cultured adipocytes (1). From these data, it may be proposed that rimonabant metabolic effects could be related, at least in part, to an enhancement of adiponectin secretion and its insulin-sensitizing actions (19). Indeed, hyperinsulinemic/euglycemic clamp studies evidenced that plasma adiponectin levels correlated significantly with insulin sensitivity in obese humans (4). The present study was aimed at investigating whether the effect of rimonabant on both body weight loss and increased insulin sensitivity required adiponectin. To that end, adiponectin ($Ad^{-/-}$) KO mice (15) and their control littermates ($Ad^{+/+}$) were fed a high-fat diet during 7 mo and treated with rimonabant or vehicle during the last month.

MATERIALS AND METHODS

Animals. The study protocol was approved by the Institutional Animal Care and Use Committee of Paris Diderot University. Adiponectin-deficient mice ($Ad^{-/-}$) were given to us by P. Froguel and T. Kadowaki. To construct the targeting vector for disruption of the adiponectin gene, a neomycin resistance gene (*neoR*) was substituted for exon 2 and exon 3, the coding region of the adiponectin gene (15). The adiponectin allele was screened by PCR from tail DNA. Duplex PCR was run using specific primers (15). All experiments were performed using littermate mice as controls ($Ad^{+/+}$).

Diet and rimonabant treatment. Mice fed ad libitum were housed under controlled temperature and lighting. Six-week-old male $Ad^{+/+}$ and $Ad^{-/-}$ mice were fed for 7 mo a 54% high-fat diet (HFD) (3) or regular chow (RC). During the last month of the diet, half of the obese mice received rimonabant daily (10 mg/kg, dilution in saline-Tween 80% by mouth, $Ad^{-/-}{}_R$ and $Ad^{+/+}{}_R$), and half received vehicle (saline-Tween 80%, $Ad^{-/-}{}_V$ and $Ad^{+/+}{}_V$).

Food intake, body weight, plasma, and liver parameters. Food intake was measured by weighing the HFD pellets every 2 days. Body weight was measured before and after vehicle or rimonabant treat-

Address for reprint requests and other correspondence: S. Migrenne, Centre National de la Recherche Scientifique-Univ. Paris Diderot-Bâtiment Buffon, 4, rue Marie Andrée Lagroua Weill-Halle-75205 Paris Cedex 13, France (e-mail: stephanie.migrenne@univ-paris-diderot.fr).

The costs of publication of this article were defrayed in part by the payment of page charges. The article must therefore be hereby marked "*advertisement*" in accordance with 18 U.S.C. Section 1734 solely to indicate this fact.

ment. Blood was sampled from caudal vessels for determination of glycemia, and plasma was collected to measure hormone using ELISA kits (insulin, leptin, and adiponectin), triglyceride (TG) and free fatty acid (FFA) concentrations. Liver TG was extracted as previously described (34). At the end, animals were killed, and subcutaneous adipose tissue (SCAT) and visceral adipose tissue (VAT) were removed and weighed.

Oral glucose tolerance test. Oral glucose tolerance tests (3 g/kg body wt) were performed in overnight fasted mice. Glycemia was monitored from a blood drop collected from caudal vessels (glucose analyzer; Roche Diagnostics, Meylan, France) at 0, 5, 10, 15, 20, 30, 40, 50, 60, 90, and 120 min, and plasma insulin was measured at 30 min. The insulinogenic index ($\Delta I/\Delta G$) was calculated by dividing the incremental plasma insulin by the incremental plasma glucose concentrations at 30 min.

Glucose turnover rate. Glucose turnover rate was assessed at the end of HFD-feeding period, using the euglycemic-hyperglycemic clamp technique. Ten days before the experiment, an indwelling catheter (Becton Dickinson, Rabalot, France) was inserted into the right jugular vein in anesthetized mice (100 mg/kg body wt ketamine/xylazine; Sigma-Aldrich, La Courneuve, France). Hyperinsulinemic-euglycemic clamp was conducted in 5-h fasted conscious mice, as previously described (29). Briefly, a 5-μCi bolus of [3-^{3}H]glucose and a priming dose of insulin (100 mU/kg; Actrapid, Novo, Copenhagen, Denmark) dissolved in isotonic saline were injected through the jugular vein, followed by a continuous infusion of [3-^{3}H]glucose (15 μCi) and insulin (6.66 $mU \cdot kg^{-1} \cdot min^{-1}$) at a constant rate of 1 μl/min to maintain blood glucose levels at 100 mg/dl. During the clamp, blood was sampled from the cut tail every 10 min to determine glucose levels and to adjust the rate of unlabeled glucose infusion to maintain euglycemia. The euglycemic conditions were reached within 30–40 min and then maintained for 60 min thereafter. Steady-state specific glucose radioactivity, plasma glucose, and insulin concentrations were determined during the last 20 min of the clamp. During the glucose clamp (50–70 min after the onset of insulin infusion), the glucose disposal rate (GDR) that reflects glucose utilization is equal to the rate of glucose appearance, resulting from hepatic glucose production (HGP), added to the amount of glucose infused necessary to maintain euglycemia (glucose infusion rate, GIR, expressed in $mg \cdot min^{-1} \cdot kg^{-1}$). For the assay of [3-^{3}H]glucose radioactivity, blood samples were deproteinized with $Ba(OH)_2$ and $ZnSO_4$, and the supernatant was evaporated to dryness at 50°C to remove tritiated water. The dry residue was dissolved in 0.5 ml water to which 10 ml scintillation solution was added (Aqualuma plus, Lumac, The Netherlands), and radioactivity was determined in a Packard Tri-Carb 460C liquid scintillation system.

Glucose utilization index (GUI) during hyperinsulinemic-euglycemic clamp. When the steady state was reached, a bolus (3 μCi) of 2-deoxy-D-[1-^{14}C] glucose (2DG; Amersham Pharmacia Biotechnology, Orsay, France) was injected by the jugular vein. Blood was sampled at time 1, 5, 10, 20, 30 40, and 60 min to measure [^{14}C]2DG specific activity. Mice were then euthanized, and tissues were collected for analysis: soleus, extensor digitorum longus, SCAT, and VAT. GUI was calculated in individual tissues from the plasma [^{14}C]2DG profile, which was fitted with a double exponential curve using Origin (OriginLab Corp, Northampton, MA) and tissue [^{14}C]2DG-6-phosphate content, as previously described (17).

Statistical analysis. Statistical analyses were performed using a two-factor repeated-measures ANOVA. Comparisons between groups were carried out using a nonpaired Student's *t*-test, except when mentioned. A *P* value of less than 0.05 was considered statistically significant.

RESULTS

Body weight and food intake. Before starting HFD feeding, $Ad^{-/-}$ mice exhibited a body weight similar to that of the wild-type $Ad^{+/+}$ mice (23.3 ± 0.5 g vs. 22.7 ± 0.5 g, ns). The HFD induced an obesity in both $Ad^{+/+}$ and $Ad^{-/-}$ mice compared with RC (Fig. 1*A*). Body weight in both $Ad^{+/+}$ and $Ad^{-/-}$ mice treated with rimonabant was significantly decreased to the same extent compared with vehicle-treated animals (Fig. 1*A*). Rimonabant had no effect on body weight in both $Ad^{+/+}$ and $Ad^{-/-}$ fed a RC compared with vehicle-treated animals (Fig. 1*A*). During the first 2 mo of HFD, the food intake in $Ad^{+/+}$ and $Ad^{-/-}$ mice increased significantly in a similar way (34 ± 3 to 58 ± 6 kcal/100 g body wt/24 h, $P < 0.001$ in $Ad^{+/+}$ mice and 37 ± 4 to 52 ± 5 kcal/100 g body wt/24 h, $P < 0.001$ in $Ad^{-/-}$ mice). Then, it stabilized during the following months of the study. Food intake was transiently decreased by rimonabant during the first week in both $Ad^{+/+}$ and $Ad^{-/-}$ mice (48.4 ± 1.4 and 34.3 ± 3.8 kcal/100 g body wt/24 h, $P < 0.01$ in vehicle and rimonabant-treated $Ad^{+/+}$ mice, respectively, and 46.1 ± 2.3 and 32 ± 2.5 kcal/100 g body wt/24 h, $P < 0.01$ in vehicle and rimonabant-treated $Ad^{-/-}$ mice, respectively). There was no difference in the weight of adipose tissue between vehicle-treated $Ad^{+/+}$ and $Ad^{-/-}$ mice fed a RC, and rimonabant treatment had no effect under these conditions (Fig. 1*B*). HFD induced an increase in fat mass in both VAT (Fig. 1*C*) and SCAT depots in $Ad^{+/+}$. In contrast, in $Ad^{-/-}$ mice, this increase was only observed in VAT. SCAT and VAT mass was decreased by rimonabant in $Ad^{+/+}$, and only VAT mass was decreased in $Ad^{-/-}$ mice compared with vehicle-treated mice (Fig. 1*C*).

Plasma and liver parameters. In RC-fed mice, all parameters were similar in $Ad^{+/+}$ and $Ad^{-/-}$ mice treated either with vehicle or rimonabant, except adiponectin, which was undetectable in $Ad^{-/-}$ mice. In HFD-fed mice, rimonabant induced a decrease in plasma FFA and TG concentrations in both $Ad^{+/+}$ and $Ad^{-/-}$ mice (Table 1). Neither the HFD nor the rimonabant treatment had an effect on TG liver content in both $Ad^{+/+}$ and $Ad^{-/-}$ mice (5.6 ± 0.9 mg TG/g liver in $Ad^{+/+}$ mice fed RC, 6.5 ± 1.9 and 7.7 ± 1.7 mg TG/g liver, ns, in vehicle and rimonabant-treated $Ad^{+/+}$ mice, respectively, and 5.8 ± 0.6 and 5.6 ± 1.7 mg TG/g liver, ns, in vehicle and rimonabant-treated $Ad^{-/-}$ mice, respectively). Both plasma leptin and insulin concentrations increased in the HFD-fed vehicle-treated $Ad^{+/+}$ and $Ad^{-/-}$ mice and decreased in $Ad^{+/+}$ and $Ad^{-/-}$ mice treated with rimonabant. Plasma adiponectin concentration decreased in the HFD-fed control $Ad^{+/+}$ compared with RC-fed $Ad^{+/+}$ mice, and rimonabant treatment increased it (Table 1).

Insulin response to oral glucose overload. Both HFD-fed $Ad^{+/+}$ and $Ad^{-/-}$ mice exhibited glucose intolerance compared with $Ad^{+/+}$ mice fed RC, and rimonabant did not improve glucose tolerance (Fig. 2, *A* and *B*). However, plasma insulin at 30 min after glucose load was markedly increased in both HFD-fed $Ad^{+/+}$ and $Ad^{-/-}$ mice compared with $Ad^{+/+}$ mice fed RC (Fig. 2*C*). Rimonabant treatment normalized insulin response in $Ad^{+/+}$ mice to the levels observed in mice fed RC but not in $Ad^{-/-}$ mice fed a HFD (Fig. 2*C*). $\Delta I/\Delta G$ was significantly increased in both vehicle-treated $Ad^{+/+}$ and $Ad^{-/-}$ mice fed a HFD (Fig. 2*D*). In $Ad^{+/+}$ mice, $\Delta I/\Delta G$ was significantly reduced by rimonabant, whereas it remained markedly increased in $Ad^{-/-}$ mice, both fed a HFD (Fig. 2*D*).

Glucose infusion rate and glucose turnover rate during hyperinsulinemic-euglycemic clamps. The HFD induced a decrease in GIR during hyperinsulinemic-euglycemic clamp (Fig. 3*A*).

GIR was significantly increased by rimonabant in $Ad^{+/+}$ mice (Fig. 3*A*) but remained unchanged in $Ad^{-/-}$ compared with vehicle-treated $Ad^{-/-}$ mice fed a HFD (Fig. 3*A*). GDR was decreased in all groups fed the HFD compared with RC-fed mice (Fig. 3*B*), and rimonabant treatment significantly increased GDR only in HFD-fed Ad+/+ mice (Fig. 3*B*). HGP

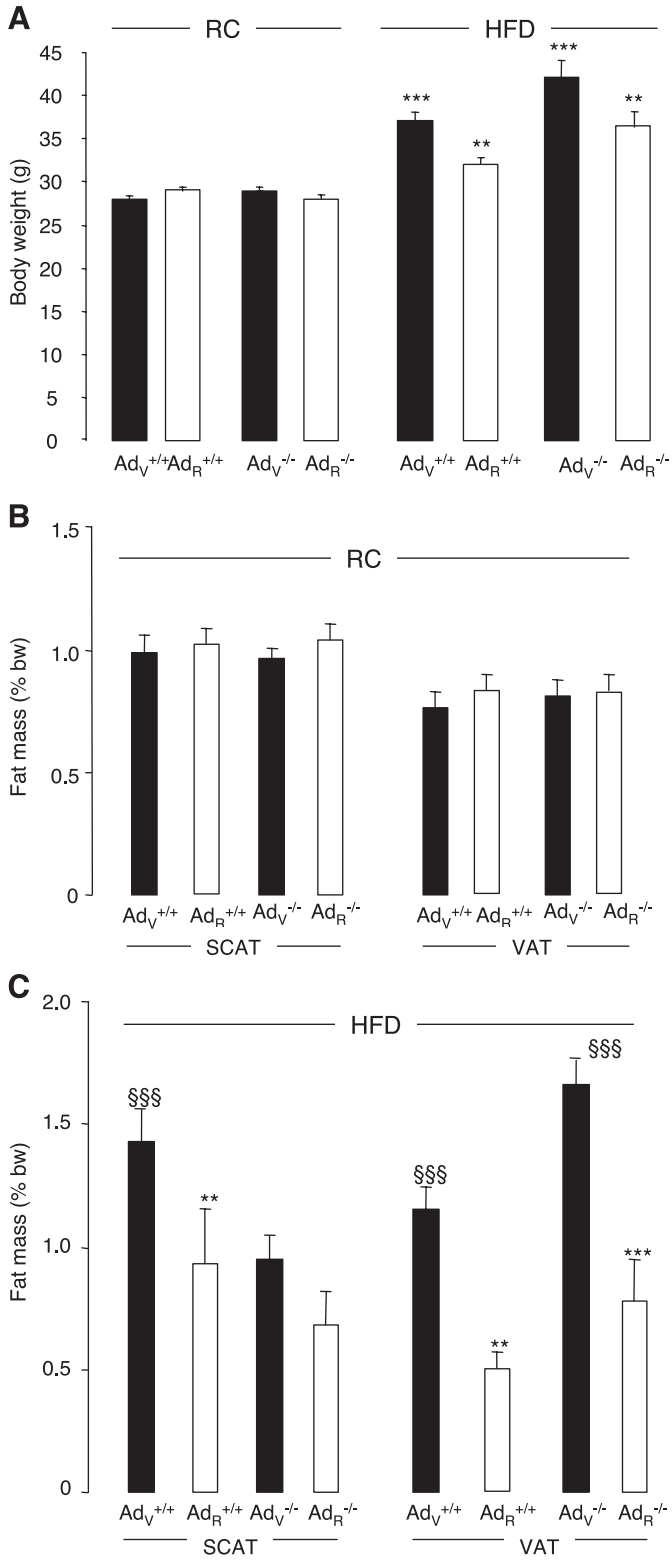

Table 1. *Plasma substrate and hormone concentration in regular chow and high-fat diet fed mice treated with vehicle or rimonabant*

	RC	HFD
Plasma triglyceride, g/l		
$Ad_V^{+/+}$	0.65±0.08	1.23±0.13‡
$Ad_R^{+/+}$	0.56±0.07	0.75±0.11†
$Ad_V^{-/-}$	0.62±0.09	1.34±0.10‡°
$Ad_R^{-/-}$	0.72±0.12	1.17±0.09*
Plasma fatty acids, μM		
$Ad_V^{+/+}$	220±38	330±52‡
$Ad_R^{+/+}$	234±27	250±48*
$Ad_V^{-/-}$	247±33	400±65‡
$Ad_R^{-/-}$	256±23	290±28*
Plasma glucose, mM		
$Ad_V^{+/+}$	7.2±0.8	9.7±0.7
$Ad_R^{+/+}$	8.0±0.7	8.4±0.6
$Ad_V^{-/-}$	8.2±0.5	8.4±0.3
$Ad_R^{-/-}$	7.8±0.7	8.2±0.3
Plasma insulin, pM		
$Ad_V^{+/+}$	234±56	364±50
$Ad_R^{+/+}$	254±43	221±37†
$Ad_V^{-/-}$	272±88	365±22
$Ad_R^{-/-}$	212±37	195±31†
Plasma leptin, nM		
$Ad_V^{+/+}$	0.45±0.03	1.30±0.22‡
$Ad_R^{+/+}$	0.52±0.06	0.72±0.20*
$Ad_V^{-/-}$	0.56±0.05	1.39±0.19‡
$Ad_R^{-/-}$	0.50±0.07	0.84±0.25*
Plasma adiponectin, μg/ml		
$Ad_V^{+/+}$	7.35±1.5	5.90±0.80‡
$Ad_R^{+/+}$	7.65±±1.2	8.20±0.67*
$Ad_V^{-/-}$	undetectable	undetectable
$Ad_R^{-/-}$	undetectable	undetectable

$Ad_R^{+/+}$ and $Ad_R^{-/-}$, wild-type and adiponectin knockout (KO) mice treated with rimonabant. $Ad_V^{+/+}$ and $Ad_V^{-/-}$, wild-type and adiponectin KO mice treated with vehicle. *$P < 0.01$, †$P < 0.001$ vs. mice treated with vehicle. ‡$P < 0.001$ vs. RC fed mice. HFD, high-fat diet; RC, regular chow. Values are expressed as means ± SD.

was significantly raised in all groups fed the HFD compared with RC-fed mice (Fig. 3*C*) and rimonabant treatment significantly reduced HGP only in HFD-fed Ad+/+ mice (Fig. 3*C*).

GUI was similar in skeletal muscles from all groups, and rimonabant treatment had no effect (Fig. 4*A*). In contrast, GUI was increased in both SCAT and VAT of rimonabant-treated $Ad^{+/+}$ but remained unchanged in rimonabant-treated $Ad^{-/-}$ mice (Fig. 4*B*).

DISCUSSION

Our data demonstrate that rimonabant's effect on body weight is adiponectin independent since it was similarly reduced in both wild-type and adiponectin KO obese mice. In contrast, unlike wild-type animals, the decrease in body weight in adiponectin KO mice was not associated with an improve-

Fig. 1. *A*: body weight of wild-type ($Ad^{+/+}$) and adiponectin knockout (KO) mice ($Ad^{-/-}$) fed a regular chow (RC) or high-fat diet (HFD) and treated with rimonabant ($Ad_R^{+/+}$ and $Ad_R^{-/-}$) or vehicle ($Ad_V^{+/+}$ and $Ad_V^{-/-}$). §§§$P <$ 0.001 vs. same group under RC diet; **$P < 0.01$ vs. vehicle treatment. *B*: Fat mass of subcutaneous (SCAT) and visceral (VAT) adipose tissue in RC fed mice. §§§$P < 0.001$ vs. RC diet; ***$P < 0.001$; **$P < 0.01$ vs. vehicle. Values are expressed as means ± SE of 9 to 12 animals in each group. *C*: Fat mass of subcutaneous (SCAT) and visceral (VAT) adipose tissue in HFD fed mice. §§§$P < 0.001$ vs. RC diet; ***$P < 0.001$; **$P < 0.01$ vs. vehicle. Values are expressed as means ± SE of 9 to 12 animals in each group.

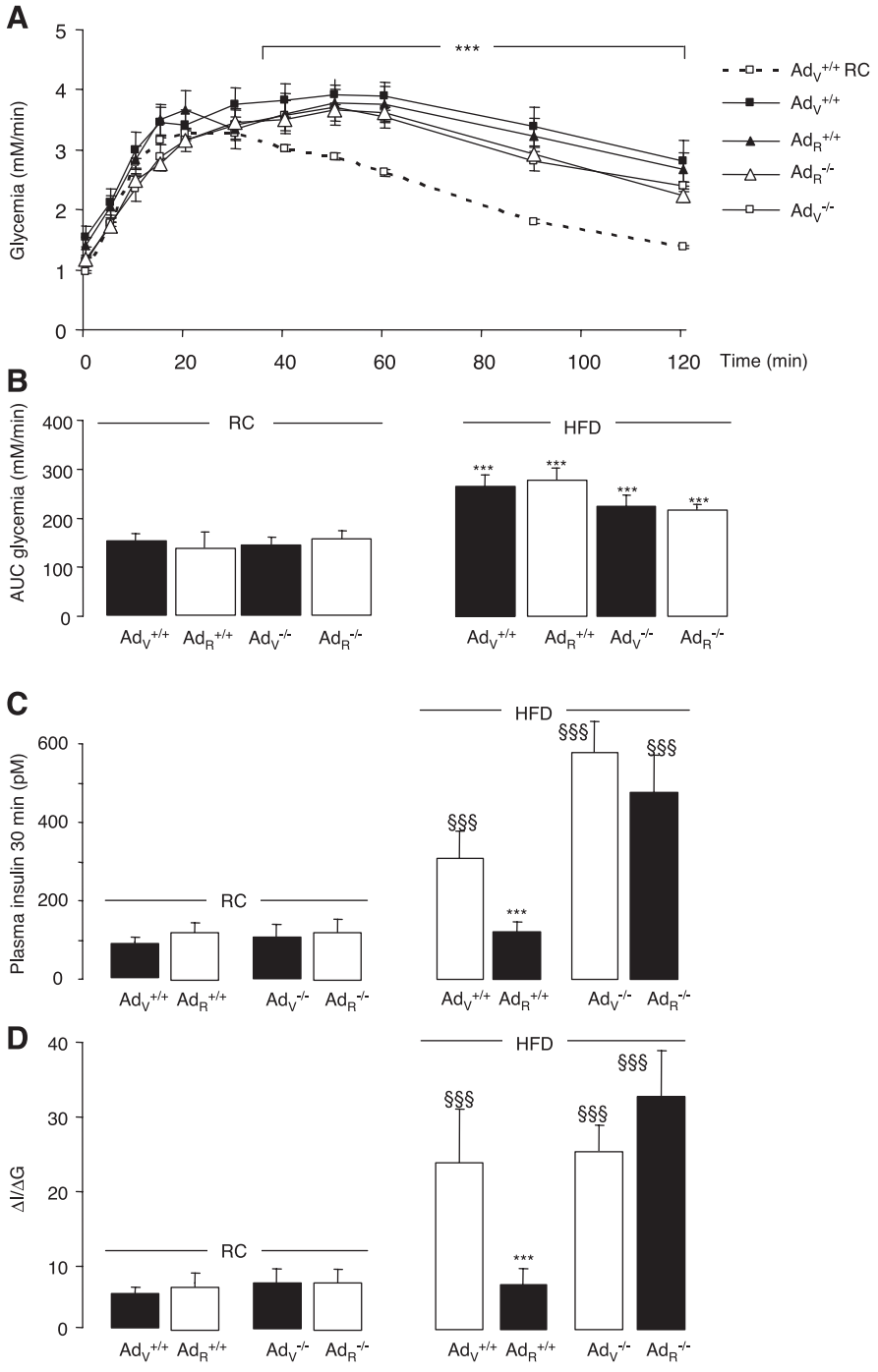

Fig. 2. *A*: time course of plasma glucose after oral glucose overload (3 g/kg body wt). Vehicle-treated $Ad^{+/+}$ mice (open square, dotted line) fed RC; Vehicle-treated $Ad^{+/+}$ (solid square), and $Ad^{-/-}$ mice (open square) fed a HFD; rimonabant-treated $Ad^{+/+}$ (solid triangle) and $Ad^{-/-}$ mice (open triangle) fed a HFD; $^{***}P < 0.001$ vs. $Ad^{+/+}$ mice fed a RC. *B*: area under the curve of glycemia during an oral glucose tolerance test (OGTT) in RC- or HFD-fed mice; $^{***}P < 0.001$ vs. $Ad^{+/+}$ mice fed a RC. *C*: plasma insulin at 30 min in RC- or HFD-fed mice; $^{§§§}P < 0.001$ vs. $Ad^{+/+}$ mice fed RC, $^{***}P < 0.001$ vs. $Ad_V^{+/+}$ fed a HFD. *D*: insulinogenic index ($\Delta I/\Delta G$) in RC- or HFD-fed mice; $^{§§§}P < 0.001$ vs. $Ad^{+/+}$ mice fed RC, $^{***}P < 0.001$ vs. $Ad_V^{+/+}$ fed a HFD. Values are expressed as means ± SE of 8 to 12 cases per group.

ment of insulin sensitivity, suggesting that the capacity of rimonabant to decrease insulin resistance requires adiponectin.

Even if rimonabant decreased body weight in both phenotypes, white adipose tissue distribution evolution pattern was different in the two groups. Indeed, HFD induced an increase in both SCAT and VAT mass in wild-type, whereas only VAT mass was increased in adiponectin KO mice. In addition, rimonabant-promoted body weight loss was associated with a decrease in both SCAT and VAT in $Ad^{+/+}$ mice, whereas VAT only was affected in $Ad^{-/-}$ mice (probably, since there is no change in SCAT mass compared with RC-fed mice). These data suggest that rimonabant action on body weight is effective only in situations with increased fat mass depots and that its effect is independent of adiponectin. This point was recently reinforced by the data of Watanabe and colleagues (32), who demonstrated that rimonabant treatment significantly decreased WAT mass and reduced the average adipocyte size to similar degrees in the *ob/ob* and *adipo*(-/-)*ob/ob* mice (32). These findings indicate that rimonabant treatment can induce a reduction of adipocyte size and thus a decrease in fat mass in the absence of adiponectin or leptin or both.

Our and other data converge to the idea of a transient decrease of food intake induced by rimonabant, whereas its effect on body weight gain and fat is persistent. This suggests

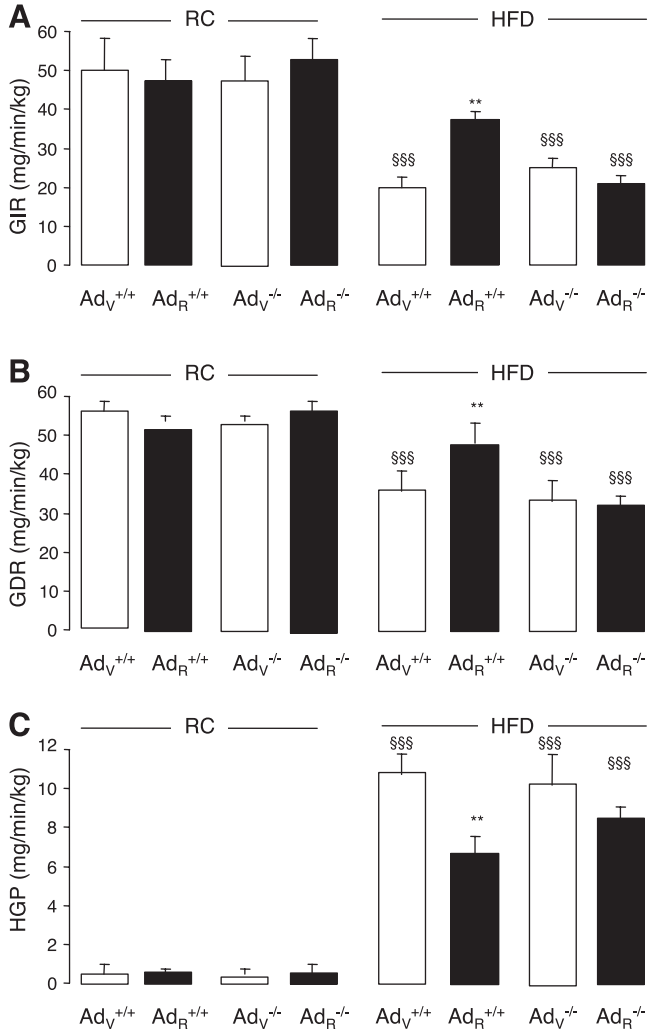

Fig. 3. *A*: glucose infusion rate (GIR). *B*: glucose disposal rate (GDR). *C*: hepatic glucose production (HGP). All three parameters were measured during hyperinsulinemic-euglycemic clamp in mice fed a regular chow (RC) or a high-fat diet (HFD) treated with rimonabant ($Ad_R^{+/+}$ and $Ad_R^{-/-}$) or vehicle ($Ad_V^{+/+}$ and $Ad_V^{-/-}$). §§§$P < 0.001$ vs. $Ad^{+/+}$ mice fed RC, **$P < 0.01$ vs. $Ad^{+/+}$ mice fed a HFD.

that, although reducing food intake may be the main initial cause for reducing body weight, it is probably not the only mechanism for the long-lasting antiobesity effect of rimonabant (22). Indeed, Liu and collaborators (16) showed that rimonabant has a direct effect on energy expenditure, suggesting that the antiobesity effect of SR141716 is due to activation of thermogenesis, in addition to the initial hypophagia. Jbilo et al. (11) showed that rimonabant activates several genes of brown adipose tissue (BAT) involved in the regulation of mitochondrial activity, and Doyon et al. (6) showed that rimonabant increased BAT UCP1 mRNA levels in obese rats. In the same way, Herling et al. (9) recently showed that the weight-reducing effect of rimonabant was due to continuously elevated energy expenditure based on increased fat oxidation driven by lipolysis from fat tissue, as long as fat stores were elevated. Finally, Tedesco et al. (28) demonstrated that CB1 receptor blockade increased mitochondrial biogenesis in white adipocytes by inducing the expression of endothelial nitric oxide synthase. This was linked to the prevention of high-fat diet-induced fat accumulation, without concomitant changes in food intake. This is of particular interest since Koh et al. (14) demonstrated that induction of increased mitochondrial biogenesis in cultured adipocytes enhanced adiponectin synthesis, suggesting a chain of cause-and-effect between rimonabant treatment and stimulation of adiponectin expression.

Glucose homeostasis was first assessed by oral glucose load in HFD-fed mice. A significant glucose intolerance associated with a compensatory insulin hypersecretion was evidenced in both $Ad^{+/+}$ and $Ad^{-/-}$ mice compared with RC-fed mice, thus suggesting a trend for an acquired peripheral insulin resistance. This phenomenon was confirmed during hyperinsulinemic-euglycemic clamp and specifically by a significantly decreased GIR in HFD-fed mice compared with their RC-fed littermates. Such insulin resistance was related to sustained hepatic glucose production and decreased glucose uptake. Rimonabant treatment had no effect on the glycemic response to glucose overload in both phenotypes. However, it normalized insulin secretion in $Ad^{+/+}$ mice, thus leading to a normalization of insulinogenic index and suggesting an improved insulin sensitivity. This was also evidenced by the increase in GIR during

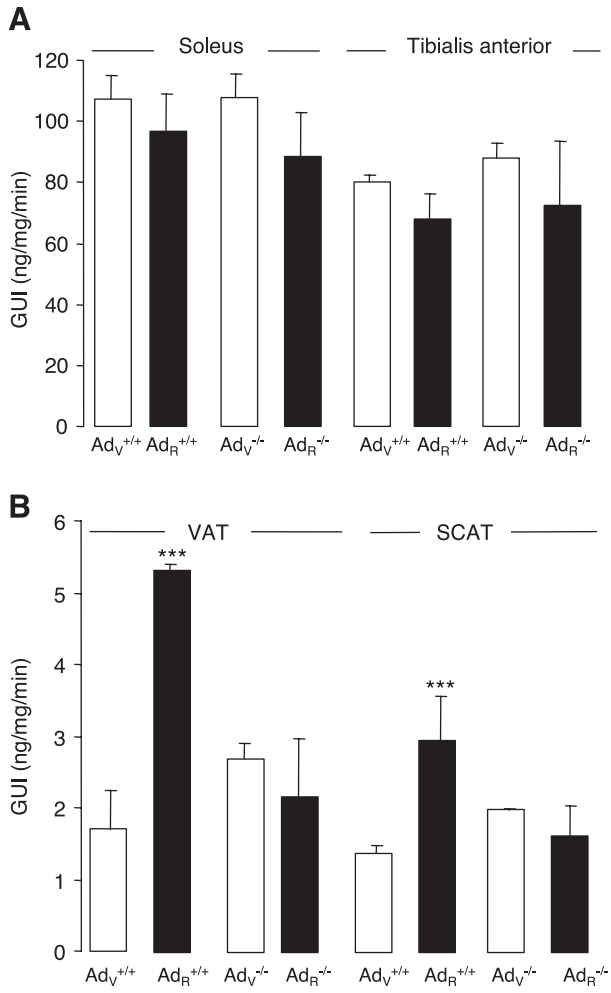

Fig. 4. *A*: glucose utilization index (GUI) in muscles of HFD-fed mice treated with rimonabant ($Ad_R^{+/+}$ and $Ad_R^{-/-}$) or vehicle ($Ad_V^{+/+}$ and $Ad_V^{-/-}$). *B*: GUI in adipose tissue (subcutaneous: SCAT or visceral VAT) of HFD-fed mice treated with rimonabant ($Ad_R^{+/+}$ and $Ad_R^{-/-}$) or vehicle ($Ad_V^{+/+}$ and $Ad_V^{-/-}$). ***$P < 0.001$ vs. vehicle-treated mice.

hyperinsulinemic-euglycemic clamp. Such an improvement of insulin sensitivity by rimonabant in $Ad^{+/+}$ mice was associated with a decreased hepatic glucose production, as well as an increase in glucose uptake mainly due to insulin-induced glucose utilization in SCAT and VAT. Contrary to Liu and collaborators (16) who showed that 7 days of rimonabant treatment (10 mg/kg ip) induced an increase in glucose uptake in isolated soleus muscle from *ob/ob* female mice, rimonabant did not increase glucose uptake in skeletal muscles of our $Ad^{+/+}$ mice. However, it is difficult to compare since it was an ex vivo study performed in female mice.

Finally, increased insulin-dependent glucose uptake evidenced by our experiments strongly suggests increased insulin signaling pathway, as also reported by Watanabe et al. (32), who showed that insulin-stimulated Akt phosphorylation was significantly increased in rimonabant-treated *ob/ob* mice compared with untreated *ob/ob* mice.

In contrast to $Ad^{+/+}$ mice, rimonabant treatment in $Ad^{-/-}$ mice did not improve insulin sensitivity, since insulinemia remained dramatically high during glucose tolerance test compared with wild-type mice. GIR was also lower in $Ad^{-/-}$ mice than in $Ad^{+/+}$ mice, demonstrating a persistent insulin resistance in spite of rimonabant treatment. However, it must be pointed out that there was a tendency to a decrease in hepatic glucose production in $Ad^{-/-}$ mice, which could be related to a reduction of both plasma TG and FFA concentrations. Indeed, in spite of adiponectin deficiency, the body weight loss induced by rimonabant was, at least in part, responsible for the decrease in plasma TG and FFA, leading to improvement of hepatic insulin sensitivity. Finally, there was no potentiation by rimonabant of insulin-mediated glucose disposal rate. This was confirmed by the absence of improvement in glucose uptake in either adipose tissue (both in SCAT and VAT) or in skeletal muscles, thus in agreement with the maintained insulin-resistant status observed in $Ad^{-/-}$ mice. In the same way, Watanabe et al. (32) demonstrated that insulin-stimulated Akt phosphorylation was impaired in the rimonabant-treated $Adipo^{-/-}$*ob/ob* mice.

Thus, our data demonstrate that rimonabant-induced insulin-sensitizing effect is mediated, at least in part, by the increase of adiponectin expression, since improvement of insulin sensitivity has been only observed in $Ad^{+/+}$-treated mice. In addition, adiponectin has been widely reported to reduce hyperinsulinemia and insulin resistance (26). Interestingly, Watanabe et al. (32) recently suggested that rimonabant treatment preferentially upregulated the expression of high-molecular-weight adiponectin, which is considered as the biologically active isoform of adiponectin, according to in vitro and in vivo data (12).

The increase in adiponectin concentration observed in $Ad^{+/+}$ mice treated with rimonabant could have also blocked the inflammatory effect induced by HFD diet. Indeed, it has been shown that adiponectin could counteract tumor necrosis factor-α (TNF-α)-mediated FFA-induced insulin resistance in 3T3-L1 adipocytes (20). It is also established that CB1 receptor is coupled to the generation of the lipid second messenger ceramide (31) involved in the induction of insulin resistance (27). In primary cultures of rat astrocytes, D9-tetrahydrocannabinol (THC) produced a rapid stimulation of sphingomyelin hydrolysis that was concomitant to an elevation of intracellular ceramide levels. These effects of THC were prevented by rimonabant (25) and interestingly, adiponectin has been evidenced to inhibit de novo ceramide synthesis through the activation of AMP kinase.

Perspectives and Significance

The present study directly demonstrates for the first time the key role of adiponectin as a mediator of rimonabant to improve insulin sensitivity, thus highlighting the importance of interplay between the cannabinoid pathway and adiponectin to regulate glucose homeostasis. This study also emphasizes the importance of a peripheral effect of rimonabant to normalize glucose homeostasis, mainly through the remodeling of adipose tissue mass.

GRANTS

This work was supported by the French Ministry of Industry and Ministry of Research through the collaborative project GenObeCB1 "Integrated genomic for obesity therapy by studying cannabinoid receptor (CB1R) and effects of its modulators".

REFERENCES

1. **Bensaid M, Gary-Bobo M, Esclangon A, Maffrand J, Le Fur G, Oury-Donat F, Soubrié P.** The cannabinoid CB1 receptor antagonist SR141716 increases Acrp30 mRNA expression in adipose tissue of obese *fa/fa* rats and in cultured adipocyte cells. *Mol Pharmacol* 63: 908–914, 2003.
2. **Blüher M, Engeli S, Klöting N, Berndt J, Fasshauer M, Bátkai S, Pacher P, Schön M, Jordan J, Stumvoll M.** Dysregulation of the peripheral and adipose tissue endocannabinoid system in human abdominal obesity. *Diabetes* 55: 3053–3060, 2006.
3. **Burcelin R, Crivelli V, Dacosta A, Roy-Tirelli A, Thorens B.** Heterogeneous metabolic adaptation of C57BL/6J mice to high-fat diet. *Am J Physiol Endocrinol Metab* 282: E834–E842, 2002.
4. **Buzzetti R, Petrone A, Zavarella S, Zampetti S, Spoletini M, Potenziani S, Leto G, Osborn J, Leonetti F.** The glucose clamp reveals an association between adiponectin gene polymorphisms and insulin sensitivity in obese subjects. *Int J Obes (Lond)* 31: 424–428, 2007.
5. **Després J, Golay A, Sjöström L, Rimonabant in Obesity-Lipids Study Group.** Effects of rimonabant on metabolic risk factors in overweight patients with dyslipidemia. *N Engl J Med* 353: 2121–2124, 2005.
6. **Doyon C, Denis RG, Baraboi ED, Samson P, Lalonde J, Deshaies Y, Richard D.** Effects of rimonabant (SR141716) on fasting-induced hypothalamic-pituitary-adrenal axis and neuronal activation in lean and obese Zucker rats. *Diabetes* 55: 3403–3410, 2006.
7. **Engeli S, Böhnke J, Feldpausch M, Gorzelniak K, Janke J, Bátkai S, Pacher P, Harvey-White J, Luft F, Sharma A, Jordan J.** Activation of the peripheral endocannabinoid system in human obesity. *Diabetes* 54: 2838–2843, 2005.
8. **Hao S, Avraham Y, Mechoulam R, Berry E.** Low dose anandamide affects food intake, cognitive function, neurotransmitter and corticosterone levels in diet-restricted mice. *Eur J Pharmacol* 31: 147–156, 2000.
9. **Herling AW, Kilp S, Elvert R, Haschke G, Kramer W.** Increased energy expenditure contributes more to the body weight-reducing effect of rimonabant than reduced food intake in candy-fed Wistar rats. *Endocrinology* 149: 2557–2566, 2008.
10. **Jamshidi N, Taylor D.** Anandamide administration into the ventromedial hypothalamus stimulates appetite in rats. *Br J Pharmacol* 134: 1151–1154, 2001.
11. **Jbilo O, Ravinet-Trillou C, Arnone M, Buisson I, Bribes E, Péleraux A, Pénarier G, Soubrié P, Le Fur G, Galiègue S, Casellas P.** The CB1 receptor antagonist rimonabant reverses the diet-induced obesity phenotype through the regulation of lipolysis and energy balance. *FASEB J* 19: 1567–1569, 2005.
12. **Kadowaki T, Yamauchi T, Kubota N, Hara K, Ueki K, Tobe K.** Adiponectin and adiponectin receptors in insulin resistance, diabetes, and the metabolic syndrome. *J Clin Invest* 116: 1784–1792, 2006.
13. **Kirkham T.** Endocannabinoids in the regulation of appetite and body weight. *Behav Pharmacol* 16: 297–313, 2005.
14. **Koh EH, Park JY, Park HS, Jeon MJ, Ryu JW, Kim M, Kim SY, Kim MS, Kim SW, Park IS, Youn JH, Lee KU.** Essential role of mitochon-

drial function in adiponectin synthesis in adipocytes. *Diabetes* 56: 2973–2981, 2007.
15. **Kubota N, Terauchi Y, Yamauchi T, Kubota T, Moroi M, Matsui J, Eto K, Yamashita T, Kamon J, Satoh H, Yano W, Froguel P, Nagai R, Kimura S, Kadowaki T, Noda T.** Disruption of adiponectin causes insulin resistance and neointimal formation. *J Biol Chem* 277: 25863–25866, 2002.
16. **Liu Y, Connoley I, Wilson C, Stock M.** Effects of the cannabinoid CB1 receptor antagonist SR141716 on oxygen consumption and soleus muscle glucose uptake in Lepob/Lepob mice. *Int J Obes* 29: 183–187, 2005.
17. **Magnan C, Gilbert M, Kahn BB.** Chronic free fatty acid infusion in rats results in insulin resistance but no alteration in insulin-responsive glucose transporter levels in skeletal muscle. *Lipids* 31: 1141–1149, 1996.
18. **Matias I, Di Marzo V.** Endocannabinoid synthesis and degradation, and their regulation in the framework of energy balance. *J Endocrinol Invest* 29: 15–26, 2006.
19. **Menzaghi C, Trischitta V, Doria A.** Genetic influences of adiponectin on insulin resistance, type 2 diabetes, and cardiovascular disease. *Diabetes* 56: 1198–1209, 2007.
20. **Nguyen MT, Satoh H, Favelyukis S, Babendure JL, Imamura T, Sbodio JI, Zalevsky J, Dahiyat BI, Chi NW, Olefsky JM.** JNK and tumor necrosis factor-alpha mediate free fatty acid-induced insulin resistance in 3T3–L1 adipocytes. *J Biol Chem* 280: 35361–35371, 2005.
21. **Piazza P, Lafontan M, Girard J.** Integrated physiology and pathophysiology of CB1-mediated effects of the endocannabinoid system. *Diabetes Metab* 33: 97–107, 2007.
22. **Ravinet Trillou C, Arnone M, Delgorge C, Gonalons N, Keane P, Maffrand JP, Soubrie P.** Anti-obesity effect of SR141716, a CB1 receptor antagonist, in diet-induced obese mice. *Am J Physiol Regul Integr Comp Physiol* 284: R345–R353, 2003.
23. **Ravinet Trillou C, Delgorge C, Menet C, Arnone M, Soubrié P.** CB1 cannabinoid receptor knockout in mice leads to leanness, resistance to diet-induced obesity and enhanced leptin sensitivity. *Int J Obes Relat Metab Disord* 28: 640–648, 2004.
24. **Ruilope L, Després J, Scheen A, Pi-Sunyer X, Mancia G, Zanchetti A, Van Gaal L.** Effect of rimonabant on blood pressure in overweight/obese patients with/without co-morbidities: analysis of pooled RIO study results. *J Hypertens* 26: 357–367, 2008.
25. **Sanchez C, Galve-Roperh I, Rueda D, Guzman M.** Involvement of sphingomyelin hydrolysis and the mitogen-activated protein kinase cascade in the Delta9-tetrahydrocannabinol-induced stimulation of glucose metabolism in primary astrocytes. *Mol Pharmacol* 54: 834–843, 1998.
26. **Sowers JR.** Endocrine functions of adipose tissue: focus on adiponectin. *Clin Cornerstone* 9: 32–40, 2008.
27. **Summers SA.** Ceramides in insulin resistance and lipotoxicity. *Prog Lipid Res* 45: 42–72, 2006.
28. **Tedesco L, Valerio A, Cervino C, Cardile A, Pagano C, Vettor R, Pasquali R, Carruba MO, Marsicano G, Lutz B, Pagotto U, Nisoli E.** Cannabinoid type 1 receptor blockade promotes mitochondrial biogenesis through endothelial nitric oxide synthase expression in white adipocytes. *Diabetes* 57: 2028–2036, 2008.
29. **Tobin V, Le Gall M, Fioramonti X, Stolarczyk E, Blazquez A, Klein C, Prigent M, Serradas P, Cuif M, Magnan C, Leturque A, and Brot-Laroche E.** Insulin internalizes GLUT2 in the enterocytes of healthy but not insulin-resistant mice. *Diabetes* 57: 555–562, 2008.
30. **Van Gaal L, Rissanen A, Scheen A, Ziegler O, Rössner S, RIO-Europe Study Group.** Effects of the cannabinoid-1 receptor blocker rimonabant on weight reduction and cardiovascular risk factors in overweight patients: 1-year experience from the RIO-Europe study. *Lancet* 365: 1389–1397, 2005.
31. **Velasco G, Galve-Roperh I, Sanchez C, Blazquez C, Haro A, Guzman M.** Cannabinoids and ceramide: two lipids acting hand-by-hand. *Life Sci* 77: 1723–1731, 2005.
32. **Watanabe T, Kubota N, Ohsugi M, Kubota T, Takamoto I, Iwabu M, Awazawa M, Katsuyama H, Hasegawa C, Tokuyama K, Moroi M, Sugi K, Yamauchi T, Noda T, Nagai R, Terauchi Y, Tobe K, Ueki K, Kadowaki T.** Rimonabant ameliorates insulin resistance via both adiponectin-dependent and adiponectin-independent pathways. *J Biol Chem* 284: 1803–1812, 2009.
33. **Woods S.** Role of the endocannabinoid system in regulating cardiovascular and metabolic risk factors. *Am J Med* 120: S19–S25, 2007.
34. **Xu H, Wilcox D, Nguyen P, Voorbach M, Suhar T, Morgan SJ, An WF, Ge L, Green J, Wu Z, Gimeno RE, Reilly R, Jacobson PB, Collins CA, Landschulz K, Surowy T.** Hepatic knockdown of mitochondrial GPAT1 in *ob/ob* mice improves metabolic profile. *Biochem Biophys Res Commun* 349: 439–448, 2006.